Published in final edited form as:
Electrochim Acta. 2013 November 1; 110: 79–85. doi:10.1016/j.electacta.2013.01.153.

The Impact of Enzyme Orientation and Electrode Topology on the Catalytic Activity of Adsorbed Redox Enzymes

Duncan G. G. McMillan[1,2], **Sophie J. Marritt**[3,4], **Gemma L. Kemp**[3,4], **Piers Gordon-Brown**[3,4], **Julea N. Butt**[3,4,5,*], and **Lars J. C. Jeuken**[1,2,*]

[1]School of Biomedical Sciences, University of Leeds, Leeds LS2 9JT, United Kingdom.

[2]School of Physics & Astronomy, University of Leeds, Leeds LS2 9JT, United Kingdom.

[3]Centre for Molecular and Structural Biochemistry, University of East Anglia, Norwich Research Park, Norwich NR4 7TJ, United Kingdom.

[4]School of Chemistry, University of East Anglia, Norwich Research Park, Norwich NR4 7TJ, United Kingdom.

[5]School of Biological Sciences, University of East Anglia, Norwich Research Park, Norwich NR4 7TJ, United Kingdom.

Abstract

It is well established that the structural details of electrodes and their interaction with adsorbed enzyme influences the interfacial electron transfer rate. However, for nanostructured electrodes, it is likely that the structure also impacts on substrate flux near the adsorbed enzymes and thus catalytic activity. Furthermore, for enzymes converting macro-molecular substrates it is possible that the enzyme orientation determines the nature of interactions between the adsorbed enzyme and substrate and therefore catalytic rates. In essence the electrode may impede substrate access to the active site of the enzyme. We have tested these possibilities through studies of the catalytic performance of two enzymes adsorbed on topologically distinct electrode materials. *Escherichia coli* NrfA, a nitrite reductase, was adsorbed on mesoporous, nanocrystalline SnO_2 electrodes. CymA from *Shewanella oneidensis* MR-1 reduces menaquinone-7 within 200 nm sized liposomes and this reaction was studied with the enzyme adsorbed on SAM modified ultra-flat gold electrodes.

Keywords

Self-assembled monolayer (SAM); protein-film electrochemistry (PFE); cytochrome; quinone; lipid vesicle

1. Introduction

Electrochemistry is a very powerful tool with which to study the catalytic mechanisms of redox enzymes [1-3]. A particularly useful method is protein-film electrochemistry (PFE), where the redox protein or enzyme is directly adsorbed on the electrode's surface. In PFE, interfacial electron transfer (ET) kinetics are not limited by diffusion of the enzyme to the electrode. When the flux of substrate to electrode is enhanced by, for instance, using a

[*]**Corresponding authors:** Lars J.C. Jeuken: School of Biomedical Sciences, University of Leeds, Leeds, UK, LS2 9JT. Tel: +44 (0)113 3433829 l.j.c.jeuken@leeds.ac.uk ; Julea N. Butt: School of Chemistry, University of East Anglia, Norwich Research Park, Norwich, UK, NR4 7TJ. Tel: +44 (0)1603 593877 j.butt@uea.ac.uk .

Europe PMC Funders Author Manuscripts

rotating-disk electrode, a platform is created in which individual steps in the catalytic cycle of enzymes can be deconvoluted. These organic-inorganic hybrid systems provide a platform for fundamental research and have application in biosensing and biofuel cells [4-6].

In order for PFE, biosensors or biofuel cells to achieve their optimal efficacy, the interfacial ET between the electrode and enzyme has to be fast compared to the enzyme's turnover. In turn, this requires the enzyme to be oriented with its electron-entry site towards the surface or, alternatively, the redox site of the enzyme can be 'wired' to the electrode [7, 8]. The orientation of enzymes physisorbed (i.e., non-covalently bound) on an electrode depends on many factors, including the charge of the electrode. For over two decades, a common and very successful approach to control the properties of a gold interface has been to modify it with self-assembled monolayers (SAMs). The influence of different SAMs on the electrochemical properties of physisorbed enzymes have been extensively investigated (e.g. ref. [9-11]). In many cases redox proteins and enzymes physisorb in a distribution of interconverting orientations that can be biased by the applied electrode potential [12-14]. Heterogeneity in the surface orientation of an adsorbed protein has been recognised to influence the electrochemical behaviour and various theories have been developed to account for distributions in electron transfer rates [1, 15].

Although the orientation of an enzyme is known to influence the interfacial ET kinetics, it is in principle possible that the turnover number of an enzyme is reduced if substrate access to the active site is obstructed by the electrode. This consideration will be especially important if enzymes have bulky substrates (e.g. polymeric substrates) or if the substrates are encapsulated in bulky entities such as lipid vesicles (Fig. 1A). It may also become significant for smaller substrates when the enzyme is adsorbed on a nanostructured electrode material (Fig. 1B). Here we present PFE of two enzymes that suggests the electrode can indeed impact on the catalytic behaviour by obstructing substrate access to the active site of these enzymes.

The impact of a mesoporous electrode material on the catalytic activity of an adsorbed enzyme film was investigated through the properties of an *Escherichia coli* periplasmic nitrite reductase, NrfA, adsorbed on mesoporous, nanocrystalline SnO_2 electrodes. NrfA contains five c-type hemes (Fig. 1B). Four of these have His/His ligation and the fifth has proximal ligation from lysine and distal ligation from water or hydroxide [16]. The lysine ligated heme is associated with the active site of NrfA where the six-electron reduction of nitrite to ammonium occurs. We have previously shown that NrfA adsorbs as an electroactive film on mesoporous, nanocrystalline SnO_2 electrodes [17, 18]. Cyclic voltammetry (CV) and spectroelectrochemistry were used to define reduction potentials for the hemes in adsorbed NrfA and the values were found to be in good agreement with those displayed by the protein in solution. Catalytic reduction was reported by CV when nitrite was included in the experiment and this confirmed the functional integrity of the adsorbed enzyme. Here, we describe how the apparent nitrite reductase activity of NrfA depends on the amount of enzyme adsorbed on the SnO_2 electrode, i.e., the enzyme coverage.

The influence of enzyme orientation on the catalytic conversion of bulky substrates was studied with CymA, which is a membrane-bound tetraheme c-type cytochrome from *Shewanella oneidensis* MR-1 (Fig. 1A). CymA contains one transmembrane α-helix localised in the inner membrane and a heme-containing globular head domain facing the periplasm. Recent characterisation of CymA by electronic absorbance, magnetic circular dichroism and electron paramagnetic resonance spectroscopies identifies three low–spin bis-histidine coordinated hemes in CymA and one high-spin heme with His/H_2O coordination [19]. We have shown that CymA can be immobilised on an electrode surface where it can catalyse the reduction of hydrophobic menaquinone-7 (MQ-7) that is located in 'bulky' lipid

vesicles [20]. Here, we aimed to control the orientation of the adsorbed CymA by changing the charge on a flat gold electrode modified with self-assembled monolayers (SAMs) of 8-mercapto-octanol (8OH) and 8-amino-1-octanethiol ($8NH_3^+$). Changes in the SAM can in principle affect the surface coverage, the interfacial electron transfer and also accessibility of enzyme to substrate and its rate of catalytic transformation. As a consequence we have monitored each of these properties separately for CymA using quartz-crystal microbalance with dissipation (QCM-D) and CV.

2. Methods

2.1 Studies of NrfA

NrfA purification and (spectro-)electrochemical characterisation after adsorption on SnO_2 electrodes were performed as described previously [16, 18]. The optically transparent SnO_2 working electrodes were comprised of a 4 μm thick layer of SnO_2 nanoparticles annealed to a fluorine-doped tin oxide coated (TEC 15) glass slide [21]. NrfA films of different surface coverage were formed by soaking SnO_2 electrodes for different times in 22.4 μM NrfA, 50 mM Hepes, 2 mM $CaCl_2$, pH 7.0. Prior to characterising the electrodes by electronic absorption spectroscopy and CV they were rinsed extensively with 50 mM Hepes, 2 mM $CaCl_2$, pH 7.0 to remove any loosely bound material. Electrochemical experiments were performed in 50 mM Hepes, 2 mM $CaCl_2$, pH 7.0 and the desired nitrite concentration while stirring the solution at 20 °C.

2.2 Studies of CymA

The preparation of ultra-flat gold electrodes (template-stripped gold), QCM-D crystals (gold surface) and CymA have been described in detail elsewhere [19, 20]. Briefly, CymA was expressed in *Shewanella oneidensis* MR-1 and purified in 0.1% n-Dodecyl β-D-maltoside (DDM) using standard chromatography methods [19]. SAMs were formed on cleaned gold electrodes by incubating them in mixtures of 8OH and $8NH_3^+$ (total concentration 1 mM) in propanol for 16 hours. It is presumed that the relative amounts of 8OH and $8NH_3^+$ in the SAM is identical to that in the solution used to make the SAM. The electrodes were incubated with either 0.1 or 0.5 μM CymA (monomer concentration) in 20 mM 3-(*N*-morpholino)propanesulfonic acid (MOPS), 30 mM Na_2SO_4, pH 7.4 (buffer) for 20 min. The CymA-modified electrode was rinsed two times with buffer supplemented with 0.01% DDM and then three times in with buffer without DDM.

The QCM-D crystals were incubated with CymA as described in the Results section, where data of the 7^{th} overtone are shown. The QCM-D frequency is converted to adsorbed mass using the Sauerbrey equation. 1-Palmitoyl-2-oleoyl-sn-glycero-3-phosphocholine (POPC) vesicles containing 1% (w/w) MQ-7 were prepared using extrusion through 200 nm track-etched membranes and added to the electrolyte at a final concentration of 1 mg/ml POPC. After incubating the CymA-modified electrodes for 20 min., the non-surface associated vesicles are removed from the electrochemical cell by rinsing with buffer. Voltammetry results indicate that a thin vesicle layer remains bound to the electrode surface. All experiments are performed inside an MBraun anaerobic glovebox with oxygen concentrations below 1 ppm at 20° C.

3. Results

3.1 PFE of NrfA on mesoporous SnO_2 electrodes

NrfA adsorbed on mesoporous, nanocrystalline SnO_2 electrodes is both electroactive and catalytically competent [17]. CV was used to quantify the amount of electroactive NrfA adsorbed on electrodes that had been soaked in a solution of 22.4 μM NrfA for different

times. The area underneath the CV peaks relates to the electroactive coverage according to Γ_{ea}= peak-area/$nFA\nu$, where Γ_{ea} is the electroactive coverage, n is the number of electrons (5 for NrfA), F the Faraday constant, A the electrode area and ν is the scan rate. The CV peaks from an electrode of geometric area 0.7 cm^2 exposed to NrfA for 18 h indicates an electroactive NrfA content of about 0.6 nmol. The effective surface area (A) of the mesoporous nanocrystalline SnO_2 electrodes is about 300× their geometric area and so the peak area equates to an electroactive NrfA coverage of about 3 pmol/cm^2, which is close to that predicted for a monolayer. Sub-monolayers of NrfA were formed by reducing the time for which the electrode was exposed to NrfA. This allowed the electroactive coverage to be varied from approximately 0.02 to 0.6 nmol/electrode (or 0.1 to 3 pmol/cm^2). There was no indication that the heme reduction potentials were dependent on the electroactive coverage.

The total amount of NrfA adsorbed on the SnO_2 electrode was also determined with electronic absorbance spectroscopy, through the Beer-Lambert law using an extinction coefficient at 410 nm of 497,650 $M^{-1}cm^{-1}$ as determined for the oxidised protein in solution [16]. The coverages determined with CV coincided with those determine spectroscopically, indicating all NrfA adsorbed on the SnO_2 is electroactive. This was further confirmed by spectroscopically assessing the oxidation state of the adsorbed NrfA [17]. With the electrode poised above 0 mV the spectrum was consistent with that of fully oxidised NrfA. At potentials below −400 mV the spectrum provided no evidence of oxidised NrfA and it was instead dominated by features typical of the reduced enzyme. Thus, all molecules of adsorbed NrfA appear to equilibrate with the applied electrode potential.

When nitrite was introduced into the voltammetric experiment clear catalytic reduction currents were observed below 0 V (Fig. 2). The catalytic current magnitude, i_{cat}, is directly related to the rate of catalysis since it quantifies electron flux through the enzyme film. The current at −600 mV approaches a limiting maximum value, i_{max}, at high nitrite concentration. For each NrfA coated electrode (containing different amounts of NrfA coverage, Γ_{ea}), the enzyme activity as a function of nitrite concentration was well-described by the Michaelis-Menten equation. This allowed the quantitation of the kinetic parameters describing catalysis, namely, K_M the Michaelis constant and i_{max}. From i_{max} and $\Gamma_{ea,}$ the maximum turnover frequency, k_{cat}, was calculated ($k_{cat} = i_{max}/6F\Gamma_{ea}$). Both k_{cat} and K_M show a clear dependence on the electroactive coverage of NrfA (Fig. 3).

3.2 PFE of CymA adsorbed on SAM-modified ultraflat gold electrodes

While the NrfA coverage on the SnO_2 electrodes was varied by changing the incubation time, CymA coverage on gold electrodes was more-conveniently varied by changing the protein concentration and the surface chemistry of the gold electrodes. Fig. 4 shows QCM-D traces for gold surfaces modified with SAMs of mixtures of 8OH/8NH_3^+ (90/10) and incubated with either 0.1 or 0.5 μM CymA (Fig. 4A and 4B, resp.). Table 1 summarises the key data for various surfaces. In general, when 8OH/8NH_3^+-modified electrodes are incubated with 0.1 μM CymA (Fig. 4A), a stable sub-monolayer forms within minutes. The sub-monolayer is resistant to washing with buffer and/or small amount of detergent (0.01% DDM). We previously reported the same behaviour when a pure 8OH SAM was incubated with 0.1 μM CymA [20]. Importantly, upon incubating the SAM with 0.1 μM CymA, the change in dissipation is negligible, which indicates that the submonolayer is rigid and the protein molecules are firmly immobilised.

When the gold surfaces are incubated with higher concentrations of CymA (0.5 μM, Fig. 4B) a more complex behaviour is observed. Initially, a multilayer of protein is formed of about two layers thick, followed by a further continuous slow adsorption, presumably forming a third layer. The dissipation rises to ~1.5×10^{-6}, consistent with a multilayer that exhibits some viscoelastic behaviour (i.e., the CymA multilayer is less rigidly coupled to the

oscillations of the QCM-D crystal). Upon rinsing the electrode with buffer (arrow '3' in Fig. 4B), a significant portion of the CymA is desorbed until approximately a monolayer remains.

For surfaces modified with mixtures of 8OH/8NH_3^+ (90/10), the electroactive coverage, Γ_{ea}, observed with cyclic voltammetry (CV) is similar to that determined with QCM-D (Table 1 and Fig. 5A). In contrast, on pure 8OH SAMs only 30-40% of the CymA on the electrode is electro-active, such that Γ_{ea} is significantly lower than found on mixed 8OH/8NH_3^+ SAMs (Fig. 5B). We propose that this is due to a different orientation of CymA predominating on 8NH_3^+-containing SAMs when compared to 8OH/8NH_3^+ SAMs. Apparently, on 8OH modified surfaces, some of the CymA enzymes are oriented such that the interfacial electron transfer rate is reduced to an extend that these enzymes are not detected anymore by CV at 10 mV/s. Fig. 6 shows the electroactive coverage as a function of 8NH_3^+ content and a maximum coverage is observed at 15% 8NH_3^+.

When the substrate of CymA, MQ-7, is supplied to the CymA-modified electrodes, a catalytic signal is observed (Fig. 7A). MQ-7 is a hydrophobic substrate and insoluble in water. Here, we have incorporated MQ-7 in phospholipid (POPC) vesicles approximately 200 nm in size. It is thus conceivable that the catalytic reduction of MQ-7 would be limited if the active site of CymA faces the electrode (Fig. 1A). The catalytic CVs are indicative for a diffusion controlled process. The fact that MQ-7 reduction is diffusion limited was previously confirmed by stirring the solution, which converts the peak shaped voltammogram to a wave [20]. The exact details of this diffusion limitation are complex. The vesicles form a thin film on the electrode and vesicle diffusion, electron transfer between MQ-7 of different vesicles and MQ-7 diffusion within a vesicle could all contribute to the observed electrochemical behaviour. The exact nature of the vesicle and MQ-7 diffusion is a topic for future studies.

In Fig. 7B, the maximum reductive current (at the peak apex) is plotted as a function of the 8NH_3^+ in the SAM. Although the catalytic signal is complex and diffusion limited, the current maximum shows a very similar dependency on 8NH_3^+ content as the electroactive coverage of CymA (compare Fig. 7B with Fig. 6). This means that to a large extent, the catalytic signal is dependent on the electroactive coverage of CymA. In Fig. 7B, the ratio between electroactive coverage and catalytic activity is used to determine k_{CymA} (=catalytic activity per CymA molecule). This shows that the catalytic activity of each CymA molecule, in addition to the electroactive coverage of CymA, is dependent on the 8NH_3^+ content of the SAM.

4. Discussion

4.1 Influence of electrode structure on catalytic activity of adsorbed enzymes

Prolonged exposure of mesoporous, nanocrystalline SnO_2 electrodes to a solution of NrfA results in close to monolayer coverage of the surface with electroactive enzyme. Shorter exposure times resulted in sub-monolayer coverage of the electrode. We presume that this is because there is less time for the NrfA to penetrate, and then adsorb to, the interior surfaces of this nanostructured mesoporous electrode material. The reduction potentials of the NrfA hemes showed no dependence on electroactive coverage. As a consequence we have no evidence to suggest that the properties of adsorbed NrfA molecules are dependent on their position within the electrode. The dependence of the catalytic parameters on electroactive coverage should then be rationalised in terms of the impact of the electrode topology on substrate access to the enzyme. Substrate (and product) molecules may not be able to diffuse effectively within the convoluted structure and this process may limit the rate of catalysis within the electrode (Fig. 1B).

NrfA molecules adsorbed deep within the mesoporous structure will encounter nitrite less frequently than those adsorbed in closest proximity to the bulk solution. As a consequence NrfA molecules deep within the structure will turnover less frequently than those in proximity to bulk solution. The rate of catalysis per molecule of adsorbed enzyme will then decrease as the coverage increases as observed for NrfA, Fig. 3A. The increase in K_M observed as the coverage of NrfA increases is consistent with this model. Higher concentrations of nitrite in the bulk solution are required to maintain a given nitrite concentration within the mesoporous structure as the electroactive coverage of NrfA increases. As a consequence catalysis by the adsorbed NrfA appears to be much less effective than it is for molecules in solution [16, 22]. Voltammetric peaks and spectroscopic features were too small to quantify electroactive coverages below 0.02 nmole NrfA/electrode. This precluded measurements to test the prediction that at sufficiently low electroactive coverage the impact of electrode topology would be negligible such that the catalytic parameters describing the properties of the adsorbed enzyme would approach those displayed by the enzyme in solution.

The optical transparency of mesoporous SnO_2 electrodes together with their capacity to accommodate high densities of adsorbed protein make them excellent materials for pursuing spectroelectrochemistry and so for determining thermodynamic properties of adsorbed enzymes with high resolution. However, here we propose that the electrode topology can hinder substrate access to the active site such that these electrodes are less informative for kinetic studies of catalysis.

4.2 Influence of SAM composition on electroactive coverage

The electroactive coverage of CymA on the surface depends strongly on the amount of $8NH_3^+$ in the SAM. This is despite the fact that the total amount of CymA on the surface is independent of the composition of the SAM. The electroactive coverage of CymA, as well as enzyme activity, shows a maximum at 15% $8NH_3^+$. We have previously reported similar studies on a copper-containing nitrite reductase (NiR), for which a maximum electroactive coverage was observed at the slightly higher $8NH_3^+$ content of 20% [23]. The activity profile of NiR as a function of $8NH_3^+$ content coincided with the measured surface capacitance of the SAM layers, which was also highest at 20% $8NH_3^+$ (see Fig. 2 in ref. [23]). We ascribed this behaviour to a depolarisation effect: dipoles of thiol molecules in a SAM interact with neighbouring molecules. For pure SAMs the net result is a depolarisation (reduction of the overall dipole) as the field of each dipole induces oppositely oriented dipoles in its neighbours. In mixed SAMs, in contrast, molecules with opposite dipoles will reinforce each other's dipoles. For $8OH/8NH_3^+$ mixtures this apparently results in the largest dipole (and possibly net positive charge on the surface) being formed at an 80/20 mixture, which in turn resulted in the highest NiR activity. Interestingly, CymA shows a clear maximum electroactive coverage (and activity) at 15% $8NH_3^+$ rather than 20%. Furthermore, at 10% $8NH_3^+$ the electroactive coverage of CymA is approximately similar to the observed coverage with QCM-D (Table 1), suggesting that under these conditions *all* CymA is oriented in an optimal conformation and the heme groups are sufficiently close to the electrode's surface to enable efficient interfacial ET. Increasing the positive charge or dipole of the SAM by increasing the $8NH_3^+$ content to 20%, results in a decrease of the electroactive coverage.

4.3 Influence of orientation on the catalytic activity

k_{CymA} shows a minimum at 15% $8NH_3^+$. Structural information of the NapC/NirT superfamily (based on the crystal structure of its homologue NrfH) indicates that two of the four hemes are surface exposed. It can thus be argued that the orientation most optimal for interfacial electron transfer is achieved when these hemes face the surface (this orientation is

shown schematically in the left hand side of Fig. 1A). Importantly, in this orientation the active site of CymA faces away from the surface and is thus accessible for lipid vesicles carrying MQ-7. As the orientation for optimal interfacial ET and substrate accessibility is predicted to coincide, it is expected that k_{CymA} should be at its maximum at 15% $8NH_3^+$, rather than at a minimum. A possible explanation for the difference between this prediction and the experimental observation could be vesicle diffusion. As the electroactive coverage increases, substrate diffusion might become relatively more limiting and k_{CymA} decreases. This effect might be enhanced by the fact that the vesicles are much larger than the enzymes. A single vesicle might interact with multiple enzymes simultaneously when the electrode is densely populated. However, detailed analysis shows that substrate diffusion cannot account for the activity observed at pure $8NH_3^+$ surfaces. While the electroactive coverage of CymA is almost identical for both pure 8OH and pure $8NH_3^+$ SAMs (difference within 5%, see insert Fig. 5), the catalytic activity is significantly higher (>20%) on the pure $8NH_3^+$ SAM (insert Fig. 6A). This difference can also not be explained by differences in the interfacial ET rate of the electroactive CymA enzymes, as this is very fast compared to the measured k_{CymA} (the interfacial ET rate at zero over-potential (k_0) is 1.5×10^3 s^{-1} for pure 8OH [20] and 140 s^{-1} for graphite electrodes [24]). We thus propose that the orientation of CymA is different on pure 8OH and $8NH_3^+$ SAMs and that this affects the ability of CymA to interact with the vesicles and thus its substrate. Due to the complicated nature of the vesicle-CymA interaction on the surface and the possible substrate-diffusion limitations, molecular details of these interactions are currently not understood in enough detail to provide further rationale for results observed here. However, even for this system, where the substrate is encapsulated in large entities (i.e., the phospholipid vesicles), the effect of orientation on enzyme-substrate interaction is rather limited and is by far exceeded by the effect that orientation has on the electroactive coverage (i.e., the relative amount of enzyme that exhibits efficient interfacial ET).

5. Conclusion

By using different enzymes and electrode systems, is has been possible to determine whether an electrode can obstruct substrate access to electrode-adsorbed enzymes. For very rough electrodes like mesoporous SnO_2, the effect of the electrode can be large and even for small substrates like nitrite, k_{cat} values can be reduced ten-fold on these electrodes. We propose that this reduction is due to hindered diffusion of the substrate to enzyme molecules adsorbed deep within the mesoporous structure of the electrode. In stark contrast, for ultrasmooth electrodes only very limited effects are observed, even when substrates are contained in bulky entities such as phospholipid vesicles. Although it is in principle possible that the electrode would shield substrate access to an enzyme if the enzyme's active site is orientated towards the electrode, no such effects were observed. Apparently, CymA retains enough mobility on the surface to allow even bulky vesicles to efficiently access its active sites.

Acknowledgments

This work was funded by the UK Biotechnology and Biological Sciences Research Council (BBSRC) and the Engineering and Physical Science Research Council (BB/G009228 and BB/C007808) and a BBSRC Ph.D. studentship to G.L.K. For the work on NrfA we are grateful to Professor James Durrant and Dr Li Xiaoe (Imperial College London, London, U.K.) for providing mesoporous nanocrystalline tin dioxide electrodes.

References

[1]. Leger C, Bertrand P. Chem. Rev. 2008; 108:2379–2438. [PubMed: 18620368]

[2]. Armstrong FA. Curr. Opin. Chem. Biol. 2005; 9:110–117. [PubMed: 15811794]

[3]. Zhang JD, Kuznetsov AM, Medvedev IG, Chi QJ, Albrecht T, Jensen PS, Ulstrup J. Chem. Rev. 2008; 108:2737–2791. [PubMed: 18620372]

[4]. Cracknell JA, Vincent KA, Armstrong FA. Chem. Rev. 2008; 108:2439–2461. [PubMed: 18620369]

[5]. Willner I, Yan YM, Willner B, Tel-Vered R. Fuel Cells. 2009; 9:7–24.

[6]. Zhou M, Dong SJ. Accounts Chem. Res. 2011; 44:1232–1243.

[7]. Katz E, Willner I. Angew. Chem.-Int. Edit. 2004; 43:6042–6108.

[8]. Noll T, Noll G. Chem. Soc. Rev. 2011; 40:3564–3576. [PubMed: 21509355]

[9]. Chen XX, Ferrigno R, Yang J, Whitesides GA. Langmuir. 2002; 18:7009–7015.

[10]. El Kasmi A, Wallace JM, Bowden EF, Binet SM, Linderman RJ. J Am Chem Soc. 1998; 120:225–226.

[11]. Leopold MC, Bowden EF. Langmuir. 2002; 18:2239–2245.

[12]. Alvarez-Paggi D, Martin DF, DeBiase PM, Hildebrandt P, Marti MA, Murgida DH. J. Am. Chem. Soc. 2010; 132:5769–5778. [PubMed: 20361782]

[13]. Jeuken LJC, Armstrong FA. J. Phys. Chem. B. 2001; 105:5271–5282.

[14]. Jin B, Wang GX, Millo D, Hildebrandt P, Xia XH. J. Phys. Chem. C. 2012; 116:13038–13044.

[15]. Jeuken LJC, McEvoy JP, Armstrong FA. J. Phys. Chem. B. 2002; 106:2304–2313.

[16]. Bamford VA, Angove HC, Seward HE, Thomson AJ, Cole JA, Butt JN, Hemmings AM, Richardson DJ. Biochemistry-Us. 2002; 41:2921–2931.

[17]. Marritt SJ, Kemp GL, Xiaoe L, Durrant JR, Cheesman MR, Butt JN. J Am Chem Soc. 2008; 130:8588–8589. [PubMed: 18549208]

[18]. Kemp GL, Marritt SJ, Li XE, Durrant JR, Cheesman MR, Butt JN. Biochem Soc T. 2009; 37:368–372.

[19]. Marritt SJ, Lowe TG, Bye J, McMillan DGG, Shi L, Fredrickson J, Zachara J, Richardson DJ, Cheesman MR, Jeuken LJC, Butt JN. Biochem J. 2012; 444:465–474. [PubMed: 22458729]

[20]. McMillan DGG, Marritt SJ, Butt JN, Jeuken LJC. J Biol Chem. 2012; 287:14215–14225. [PubMed: 22393052]

[21]. Topoglidis E, Astuti Y, Duriaux F, Gratzel M, Durrant JR. Langmuir. 2003; 19:6894–6900.

[22]. Angove HC, Cole JA, Richardson DJ, Butt JN. J Biol Chem. 2002; 277:23374–23381. [PubMed: 11970951]

[23]. Krzeminski L, Cronin S, Ndamba L, Canters GW, Aartsma TJ, Evans SD, Jeuken LJC. J Phys Chem B. 2011; 115:12607–12614. [PubMed: 21939276]

[24]. Firer-Sherwood M, Pulcu GS, Elliott SJ. J. Biol. Inorg. Chem. 2008; 13:849–854. [PubMed: 18575901]

[25]. Rodahl M, Hook F, Fredriksson C, Keller CA, Krozer A, Brzezinski P, Voinova M, Kasemo B. Faraday Discuss. 1997; 107:229–246. [PubMed: 9569776]

Europe PMC Funders Author Manuscripts

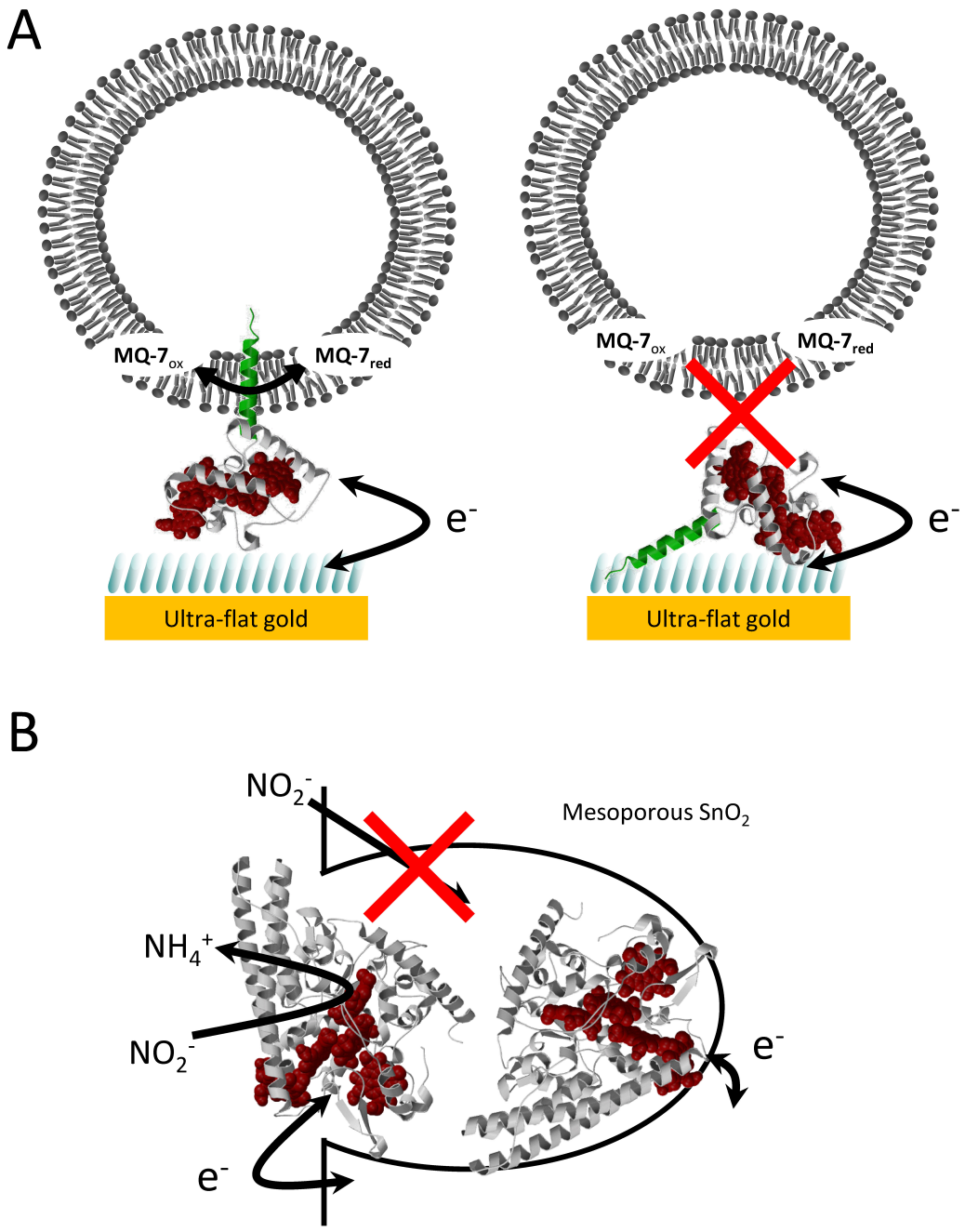

Fig. 1. Schematics of the protein film electrochemistry pursued in this work.

(A) A ribbon presentation of NrfH, a homologue of CymA, immobilised on a SAM modified gold electrode together with a lipid vesicle with MQ-7. The 8OH and $8NH_3^+$ thiols in the SAM are shown as blue bars, the NrfH polypeptide in white (globular 'head' domain), green (lipophilic 'tail') and red (the prosthetic heme groups). Two possible orientations for the adsorption of CymA are illustrated. (B) A ribbon presentation of NrfA adsorbed within a mesoporous, nanocrystalline SnO_2 electrode with the polypeptide in white and hemes in red.

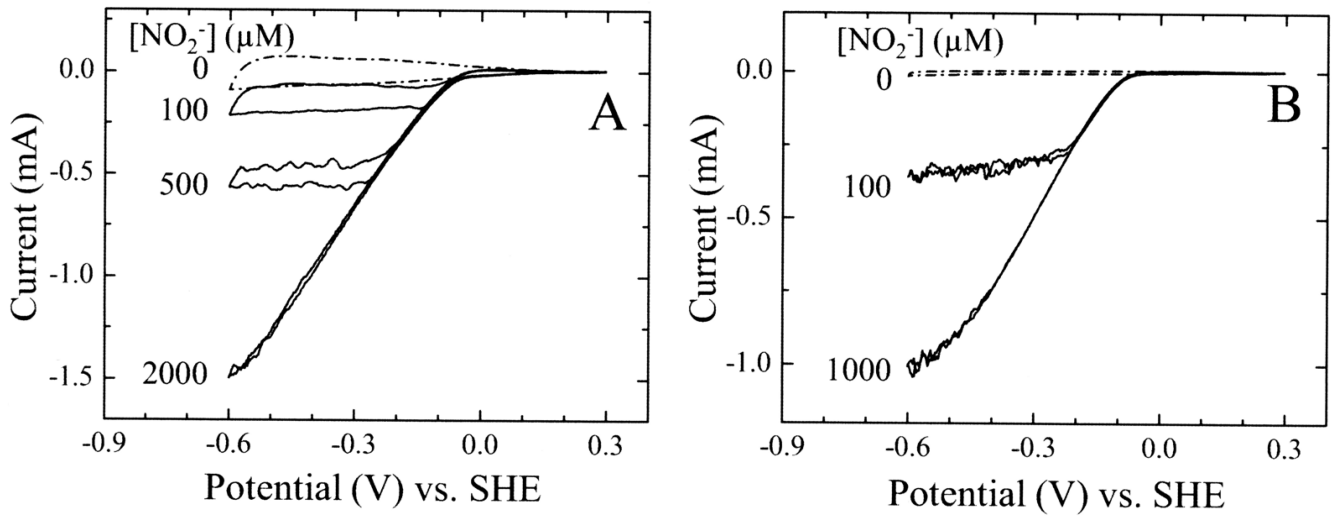

Fig. 2. Baseline corrected CVs of NrfA adsorbed on mesoporous, nanocrystalline SnO_2 electrodes at the indicated nitrite concentrations.

Electroactive coverage of NrfA: (A) 0.56 nmol/electrode and (B) 0.02 nmol/electrode. Scan rate 30 mV/s in 50 mM Hepes, 2 mM $CaCl_2$, pH 7.

Europe PMC Funders Author Manuscripts

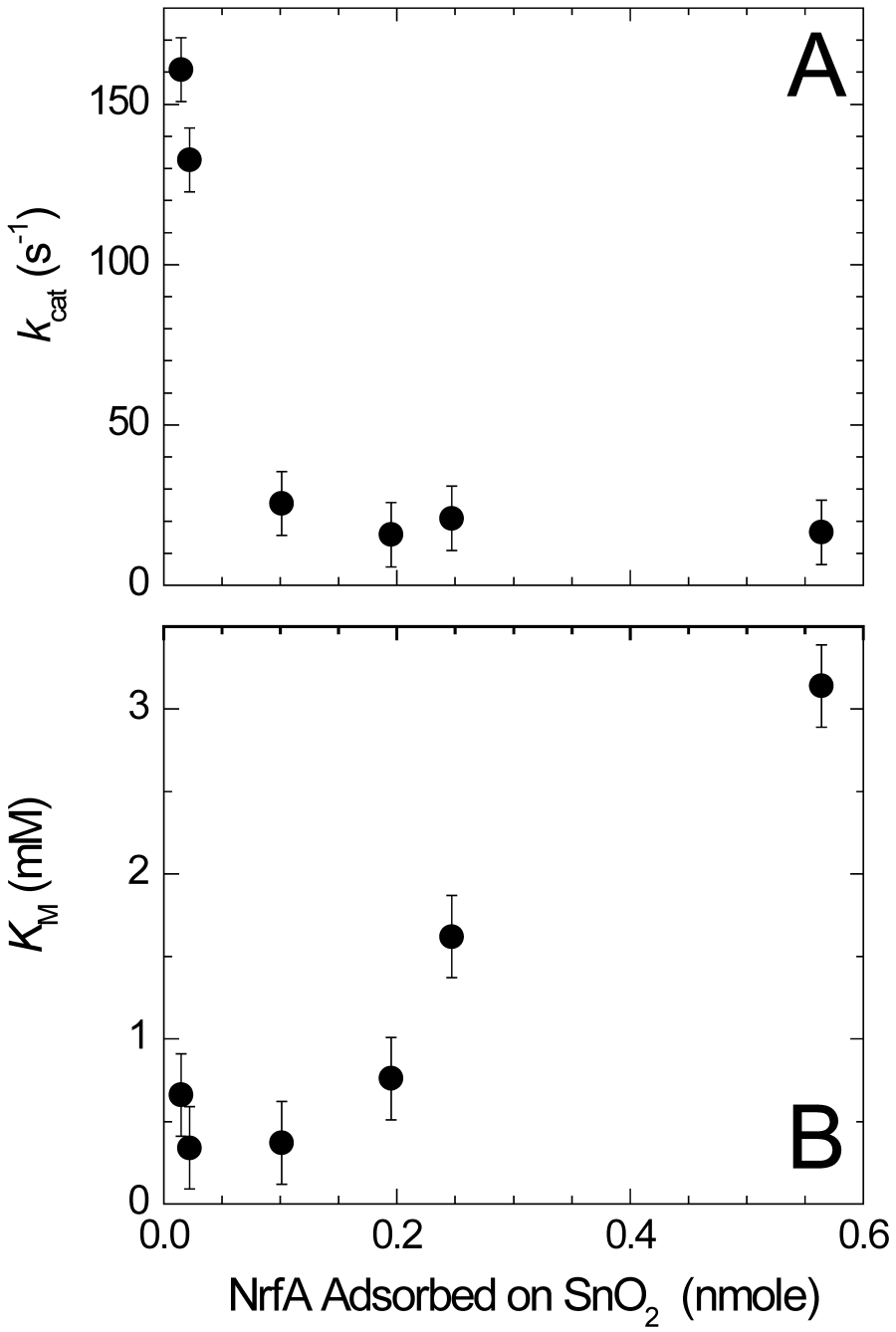

Fig. 3. Variation of k_{cat} and K_M for NrfA nitrite reduction as a function of the electroactive coverage of NrfA adsorbed on the mesoporous SnO_2 electrode.

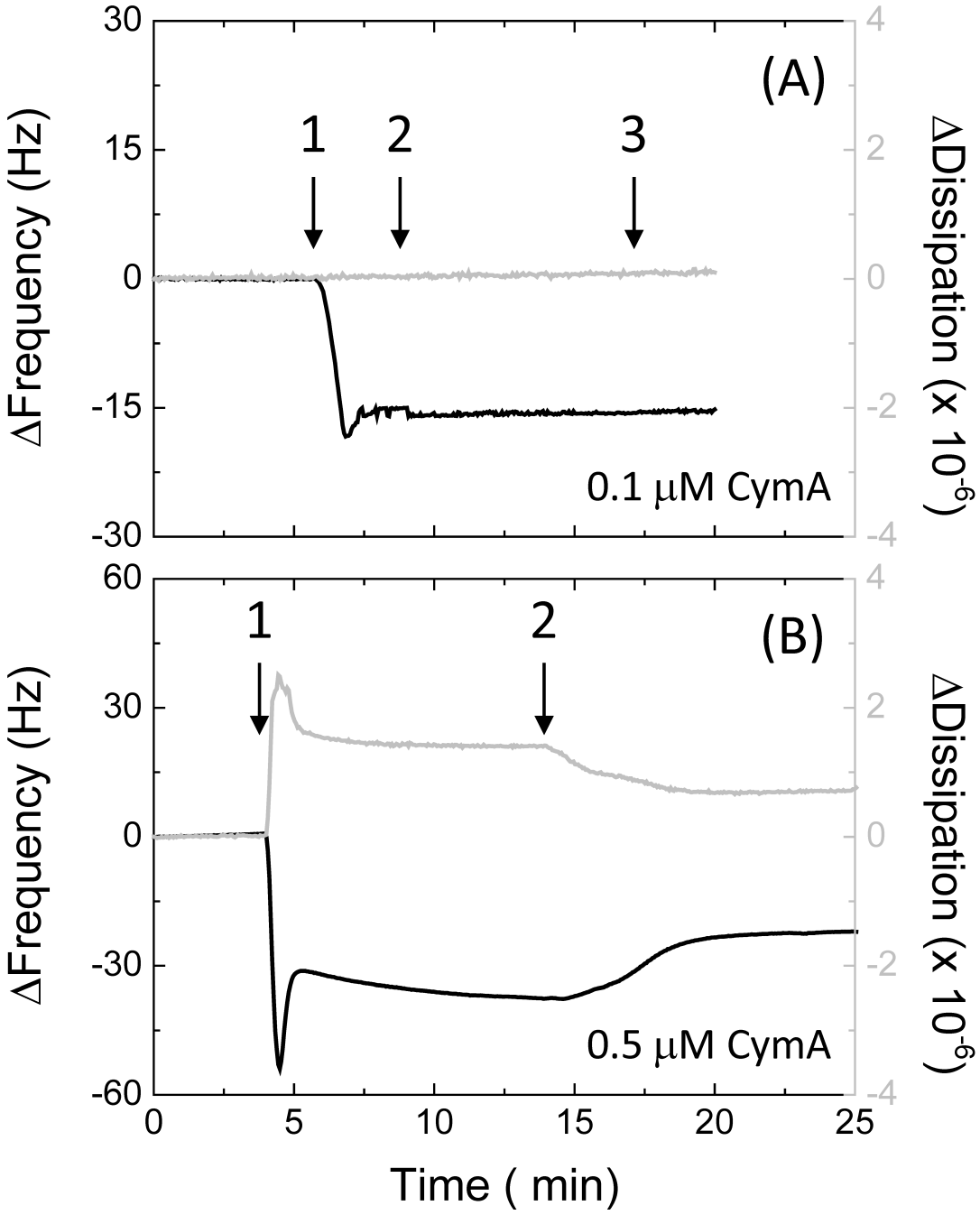

Fig. 4. QCM-D results in buffer with frequency (black line, left axis) and dissipation (grey line, right axis) against time for (A) a 8OH/8NH_3^+ (90/10) and (B) a pure 8OH modified gold surface.
Time points: **1**, (A) 0.1 and (B) 0.5 μM CymA in buffer; **2**, buffer only; **3**, CV between 0.5 and −0.4 V versus SHE at 10 mV/s. The plots shown are representative of triplicate experiments.

Europe PMC Funders Author Manuscripts

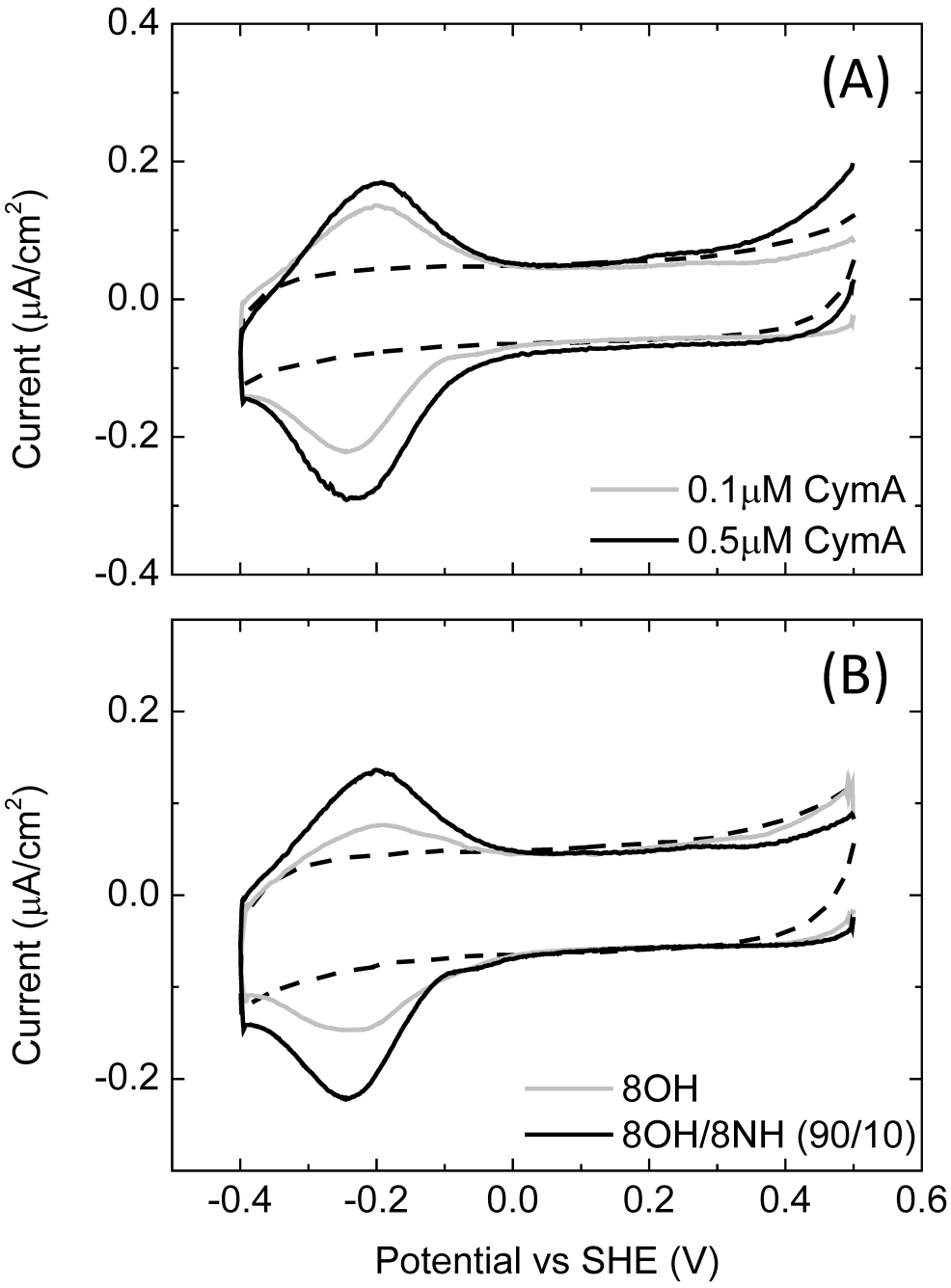

Fig. 5. (A) CVs (10 mV/s) of 8OH/8NH$_3^+$ (90/10) modified gold electrode in buffer, incubated with 0.1 or 0.5 μM CymA, as indicated. (B) CVs (10 mV/s) of 8OH or 8OH/8NH$_3^+$ (90/10) modified gold electrodes, as indicated.

The CV are measured in buffer after incubation with 0.1 μM CymA. The dashed lines in (A) and (B) are CVs before incubation with CymA.

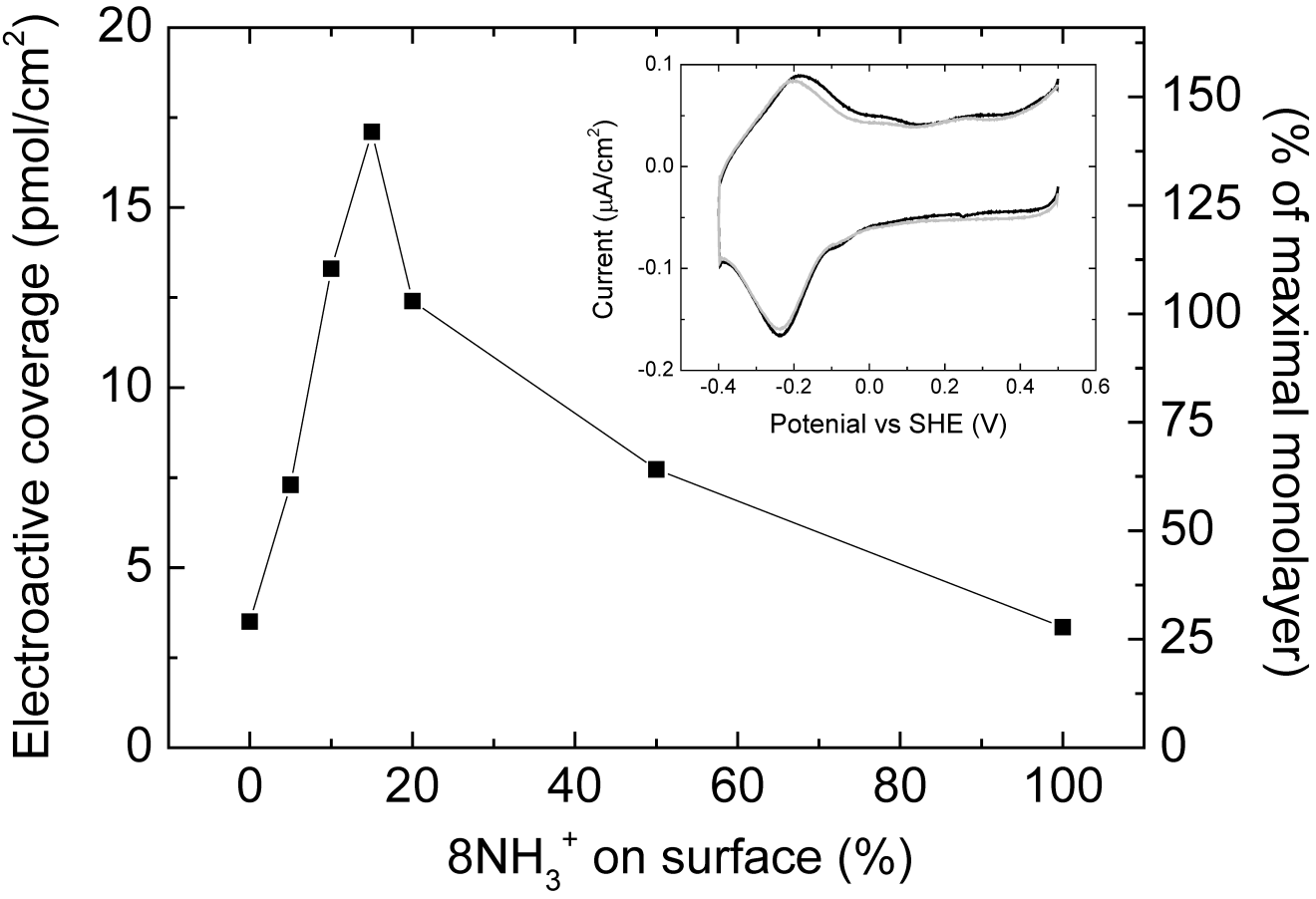

Fig. 6. Electroactive coverage as determined by CV as a function of relative amount of $8NH_3^+$ on the surface, which is given as $8NH_3^+/(8NH_3^+ + 8OH)$.

The surfaces were incubated with 0.5 μM CymA. (Insert) CVs (10 mV/s) of (black line) pure 8OH and (grey line) pure $8NH_3^+$ modified gold electrode in buffer, incubated with 0.5 μM CymA.

Europe PMC Funders Author Manuscripts

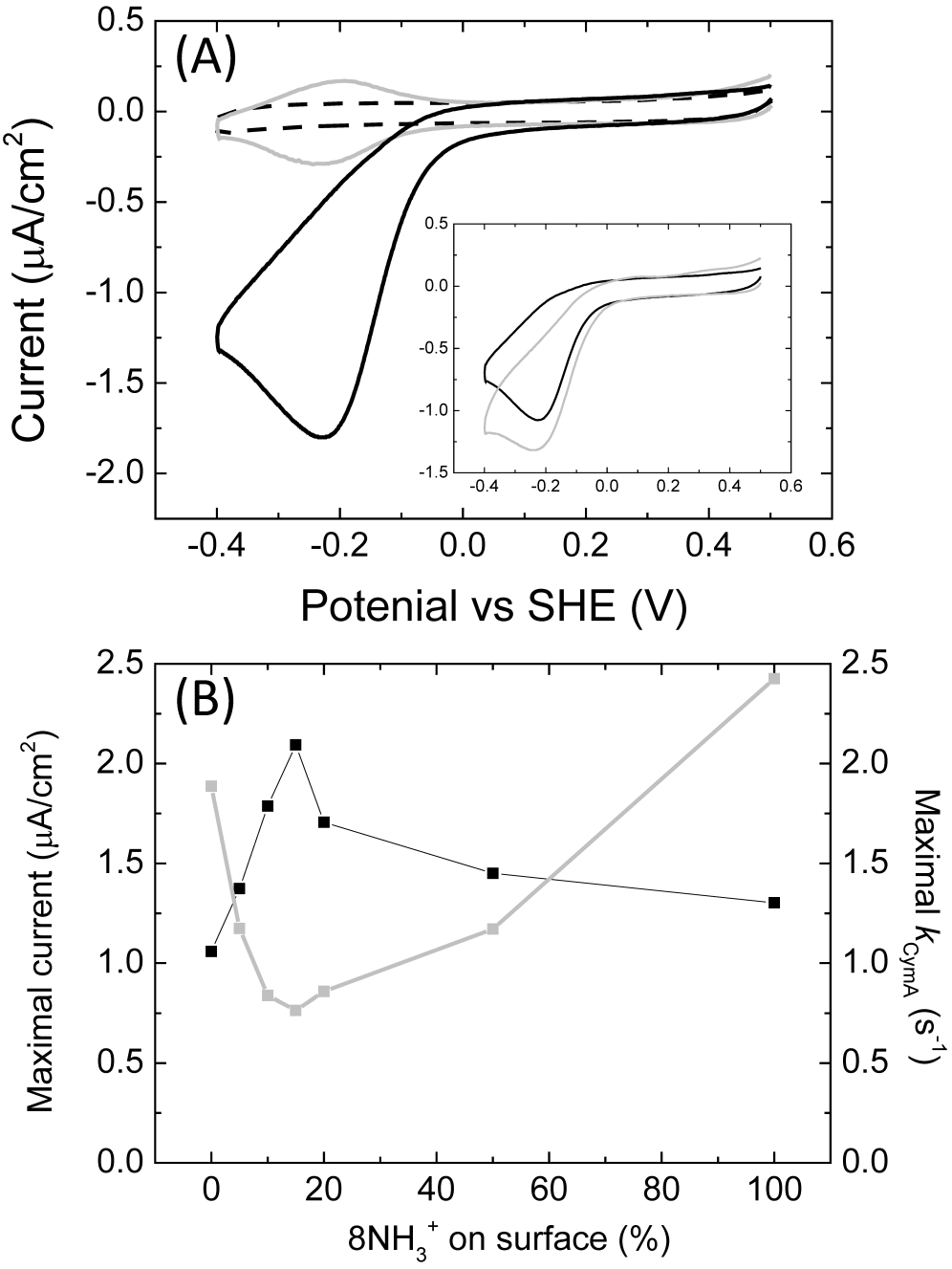

Fig. 7. (A) CVs (10 mV/s) of 8OH/8NH_3^+ (90/10) modified gold electrode in buffer, incubated with 0.5 μM CymA before (grey line) and after (black line) addition of POPC vesicles containing 1.0% (w/w) MQ-7. The dashed line is a CV before incubation with CymA. (Insert) idem, for (black line) pure 8OH and (grey) pure 8NH_3^+ modified surfaces. (B) Black line: The maximum current determined at about −0.2 V vs SHE from CVs such as shown in (A) as a function of the relative amount of 8NH_3^+ on the surface, which is given as 8NH_3^+/(8NH_3^+ + 8OH). Grey line: k_{CymA} (= the activity per CymA enzyme) as a function of the relative amount of 8NH_3^+ on the surface.

Table 1

Summary of the CymA coverage on various surfaces as determined with QCM-D and voltammetry.

Values given in percentages are ± 10% and rounded to the nearest 10%. Coverage determined by QCM-D are ± 0.03 μg/cm^2 and coverages determined by cyclic voltammetry are ± 1 pmol/cm^2.

SAM (8OH/8NH$_3^+$)	Conc. (μM) [a]	QCM-D		Cyclic voltammetry		Fraction of coverage that is electroactive
		(μg/cm^2)	% [b]	pmol/cm^2	% [c]	
100/0	0.1	0.24	70%	3.5	30%	40%
100/0	0.5	0.35	110%	3.5	30%	30%
90/10	0.1	0.24	70%	7	50%	70%
90/10	0.5	0.35	110%	13	110%	100%

[a] The concentration of CymA that is used to form a CymA film. In each case, the electrode is incubated with CymA for 20 min. at 20° C.

[b] This column shows the relative coverage as a percentage of a dense monolayer of CymA (12 pmol/cm^2), which is calculated using the approximate protein size (taken from a crystal structure of a CymA homologue, NrfH) and assuming that 30% of the adsorbed mass is due to water associated with the protein film (total weight: 12 pmol × 20.8 kDa × 1.3 = 0.33 μg/cm^2) [25].

[c] This column shows the relative coverage as a percentage of a calculated monolayer of CymA (= 12 pmol/cm^2), which is calculated using the approximate protein size (taken from a crystal structure of a CymA homologue, NrfH).